Panoramic stereo photography based on single-lens with a double-symmetric prism

Chien-Yue Chen,[1,*] Qing-Long Deng,[2] Wen-Shing Sun,[3,5] Qiao-Yao Cheng,[3] Bor-Shyh Lin,[4] and Ching-Lung Su[1]

[1]*Graduate School of Optoelectronics, National Yunlin University of Science &Technology, 64002 Douliou Yunlin, Taiwan*
[2]*Institute of Photonic Systems, National Chiao Tung University, Tainan 71150, Taiwan*
[3]*Department of Optics and Photonics, National Central University, 32001 ChungLi Taoyuan, Taiwan*
[4]*Institute of Imaging and Biomedical Photonics, National Chiao Tung University, Tainan 71150, Taiwan*
[5]*wssun@dop.ncu.edu.tw*
[*]*chencyue@yuntech.edu.tw*

Abstract: Different from traditional panorama stereo acquisition technique shooting with numerous cameras, this study equips a double-symmetric prism in front of a single-lens camera to acquire images from four different angles of view, and the images acquired from the cameras every 20 degrees complete a pair of panorama stereo images with vertical angle of view (± 16 degrees) by image-based rendering. The panorama stereo acquisition technique reduces the number of cameras by three-fourth, and the acquired images contain vertical angles of view. Moreover, the image resolution is enhanced several times of the resolution of integral photography without moiré effect.

OCIS codes: (110.6880) Three-dimensional image acquisition; (120.4820) Optical systems; (220.4830) Systems design.

References and links

1. D. M. Hoffman, A. R. Girshick, K. Akeley, and M. S. Banks, "Vergence-accommodation conflicts hinder visual performance and cause visual fatigue," J. Vis. **8**(3), 1–30 (2008).
2. S. Y. Park, N. Lee, and S. Kim, "Stereoscopic imaging camera with simultaneous vergence and focus control," Opt. Eng. **43**(12), 3130–3137 (2004).
3. S. J. Watt, K. Akeley, M. O. Ernst, and M. S. Banks, "Focus cues affect perceived depth," J. Vis. **5**(10), 834–862 (2005).
4. T. P. Pachidis and J. N. Lygouras, "Pseudo-stereo vision system: A detailed Study," J. Intell. Robot. Syst. **42**(2), 135–167 (2005).
5. J. Gluckman and S. K. Nayar, "Rectified catadioptric stereo sensors," IEEE Trans. Pattern Anal. Mach. Intell. **24**(2), 224–236 (2002).
6. J. Zhu, Y. Li, and S. Ye, "Design and calibration of a single-camera-based stereo vision sensor," Opt. Eng. **45**(8), 083001 (2006).
7. Y. Xiao and K. B. Lim, "A prism-based single-lens stereovision system: From trinocular to multi-ocular," Image Vis. Comput. **25**(11), 1725–1736 (2007).
8. D. H. Lee and I. S. Kweon, "A novel stereo camera system by a biprism," IEEE Trans. Robot. Autom. **16**(5), 528–541 (2000).
9. C. Y. Chen, T. T. Yang, and W. S. Sun, "Optics system design applying a micro-prism array of a single lens stereo image pair," Opt. Express **16**(20), 15495–15505 (2008).
10. S. Peleg, M. Ben-Ezra, and Y. Pritch, "Omnistereo: panoramic stereo imaging," IEEE Trans. Pattern Anal. Mach. Intell. **23**(3), 279–290 (2001).
11. S. E. Chen and L. Williams, "Quicktime VR-an image-based approach to virtual environment navigation," in *SIGGRAPH'95*, (Association for Computing Machinery, Los Angeles, 1995), pp. 29–38.
12. L. McMillan and G. Bishop, "Plenoptic modeling: an image-based rendering system," in *SIGGRAPH'95*, (Association for Computing Machinery, Los Angeles, 1995), pp. 39–46.
13. Y. C. Chen, C. F. Chang, and Z. N. Shen, "Image-based model acquisition and interactive rendering for building 3D digital archives," in *Proceedings of 2005 International Conference on Digital Archives Technologies* (ICDAT 2005).
14. F. Okano, H. Hoshino, J. Arai, and I. Yuyama, "Real-time pickup method for a three-dimensional image based on integral photography," Appl. Opt. **36**(7), 1598–1603 (1997).
15. T. Naemura, T. Yoshida, and H. Harashima, "3-D computer graphics based on integral photography," Opt. Express **8**(4), 255–262 (2001).

#185526 - $15.00 USD Received 19 Feb 2013; revised 21 Mar 2013; accepted 23 Mar 2013; published 29 Mar 2013

16. H. Hoshino, F. Okano, H. Isono, and I. Yuyama, “Analysis of resolution limitation of integral photography,” J. Opt. Soc. Am. A **15**(8), 2059–2065 (1998).
17. M. Okui, M. Kobayashi, J. Arai, and F. Okano, “Moiré fringe reduction by optical filters in integral threedimensional imaging on a color flat-panel display,” Appl. Opt. **44**(21), 4475–4483 (2005).
18. W. J. Smith, in *Modern Optical Engineering* (Mc Graw Hill, 2008), pp.123–125.
19. J. K. Hasegawa and C. L. Tozzi, “Shepe from Shading with perspective projection and camera calibration,” Comput. Graph. -UK **20**(3), 351–364 (1996).
20. B. Julesz, “Cyclopean perception and neurophysiology,” Invest. Ophthalmol. **11**(6), 540–548 (1972).

1. Introduction

With the development of binocular parallax-based left and right image acquisition [1], the stereo acquisition techniques have been divided into dual-lens and single-lens [2] techniques in order to acquire the stereo depth of a real object. Having two identical cameras allows dual-lens stereo acquisition, where the left image of the object from the left angle of view is imaged by the left camera, while the right one is imaged by the right camera. The depth of the object can be calculated by the disparity between the left and the right images [3]. Nevertheless, the two cameras are required to be of identical specification and the disparity of circuit triggering frequency for shooting dynamic contents should be lower than 10fps to prevent the left and the right images from asynchrony. The simplified single-lens stereo acquisition technique improves upon the above problems. The simplified single-lens stereo acquisition technique is divided into reflective lens [4,5] and refractive lens [6,7] techniques. The refractive single-lens acquisition technique simply places a biprism in front of a charge-coupled device (CCD) for the images from the left and the right angles of view [8] so that the complicated optical path is largely reduced when compared to the reflective one. However, the thick biprism is not easily coupled with CCDs. Chen *et. al* (2008) proposed to replace the biprism in a single-lens stereo camera with a micro prism array, reducing about 90% of the volume, which was further applied to a zoom system [9].

On the other hand, in addition to retaining the stereo image with actual depth, stereo acquisition needs to meet the requirement of panorama stereo images, presenting all scenes in a 3D space [10]. The past acquisition, named Image-based rendering (IBR) [11], depended on several cameras acquiring a static object from various tangents and completing a panorama stereo image by back-end computing. The combined panorama stereo image, as the three-dimensional image of the object [12,13], was then rebuilt on the display with circular projections [10] so that the audience could freely select the angles from which to view the object. Nonetheless, the common acquisition angles were fixed horizontally so that merely the horizontal images could be acquired, but not the vertically stereo type. To present the stereo information of the target from various angles or the dynamic scenes, the hardware equipment would be increased so that asynchronous signal errors would be increased and further affect the image linking. Integral photography (IP), which placed the lens array in front of the lens, was then gradually developed [14,15]. The number of cameras was reduced, but the resolution was also tremendously reduced [16], and some moiré effect appeared [17].

In this case, this study proposes a binocular parallax-based single-lens stereo acquisition technique with multi-angle of view, designs a double-symmetric prism being equipped in front of the single-lens camera, and proceeds panorama acquisition by placing cameras at every 20 degrees. After one acquisition, each camera would acquire images from four different angles of view (2 × 2 angle of view), which are calculated with IBR and binocular parallax for two sets of panorama stereo images from the upper and the lower angles of view (longitudinal axis), and each panorama stereo image contains 18 stereo image pairs (latitude axis). Since there are two horizontal images, the images from the left and the right angles of view could be obtained from one acquisition; therefore, half of the cameras could be deleted when compared to traditional acquisition. The acquired images conform to the actual viewing with binocular parallax so that crosstalk is not caused. Meanwhile, the vertical angles of view, about ± 16 degrees, are increased, and 1/4 image resolution is enhanced several times of the resolution of IP without the moiré effect.

#185526 - $15.00 USD Received 19 Feb 2013; revised 21 Mar 2013; accepted 23 Mar 2013; published 29 Mar 2013

2. Principle

Figure 1 shows the optic path of a single-lens camera for the proposed panorama stereo acquisition technique. When the double-symmetric prism is placed in front of the single-lens camera, the horizontal half-angle of view $\theta_{\omega(H)}$ and the vertical half-angle of view $\theta_{\omega(V)}$ of the chief ray of the Lens are refracted through the prism, changing the maximum width ($\delta_{w(H)}$, $\delta_{w(V)}$) for acquisition, and the incident angle ($\delta_{o(H)}$, $\delta_{o(V)}$) of marginal ray has approach the optic axis. The refracted chief ray and marginal ray therefore could be divided into four collection areas. In other words, the left and the right angles of view on the latitude axis and the upper and the lower angles of view on the longitude axis of the target, after passing through the prism and lens, are collected to a CCD, presenting quadrants.

Based on the prism principle [18], the change of emergent light after the incident light from various angles passing through the prism is presented, and the equations for the marginal ray and the chief ray in the system are re-defined. First, the clockwise direction including the angle between the light and the normal is defined as positive, while the counterclockwise one is defined as negative; and, the clockwise direction including the angle between the light and the optic axis is defined as positive, while the counterclockwise one is defined as negative. When the light from the incident angle δ_o is being refracted by the prism, the emergent light parallels the optic axis Z, and the included angle between the emergent light and the normal on the incline of the prism equals the vertex angle α of the prism, as shown in Fig. 2(a), so that Eq. (1) for the marginal ray is defined. Similarly, when the light from the incident angle δ_ω is being refracted by the prism, the included angle between the emergent light and the optic axis Z is the half-angle of view θ_ω of the lens, and the emergent angle θ_2 is the sum of the vertex angle α and the half-angle of view θ_ω so that Eq. (2) for the chief ray is defined.

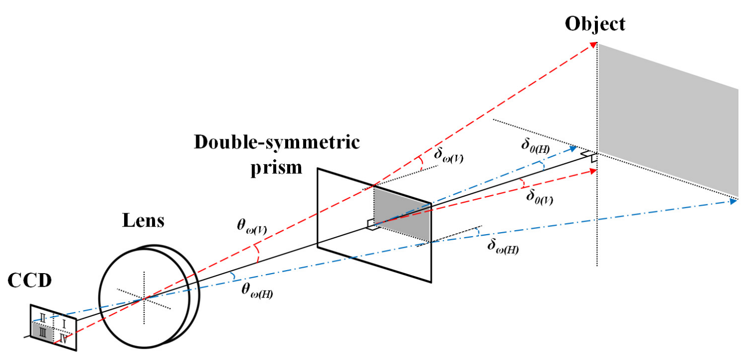

Fig. 1. Optic path of the single-lens camera for the panorama stereo acquisition technique.

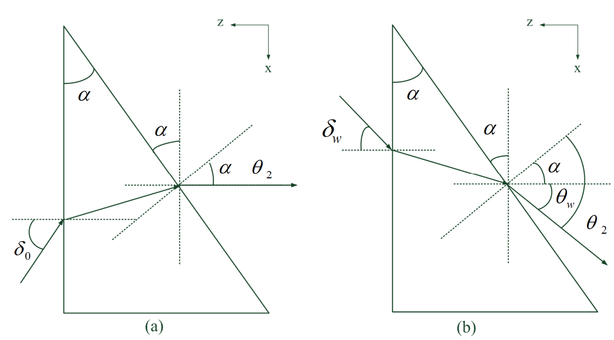

Fig. 2. The collect cone angles δ_o and δ_ω of the system: (a) marginal ray; (b) chief ray.

#185526 - $15.00 USD Received 19 Feb 2013; revised 21 Mar 2013; accepted 23 Mar 2013; published 29 Mar 2013

$$\delta_o = \sin^{-1}(\sin\alpha(n^2 - \sin^2\alpha)^{1/2} - \cos\alpha\sin\alpha) \quad (1)$$

$$\delta_\omega = \sin^{-1}\{\cos\alpha\sin(\alpha - \theta_\omega) - \sin\alpha[n^2 - \sin^2(\alpha - \theta_\omega)]^{1/2}\} \quad (2)$$

2.1 Lens design

As the half-angle of view of the lens determines the acquisition area, a CCD with 1/2” progressive scan CCD is selected for acquiring the angle of view corresponding to the binocular parallax, and an optical software *ZEMAX* is utilized for optimizing the horizontal half-angle of view ($\theta_{\omega(H)}$) and the vertical half-angle of view ($\theta_{\omega(V)}$). The specification is shown in Table 1 and Fig. 3. Subsequently, MTF, distortion, and relative illumination are applied to inspect the image quality of the lens. About the MTF change from field of view and spatial frequency, the minimum 46% of the tangential rays appear at the field of view 45 lps/mm (image height 2.76 mm), as shown in Fig. 4(a). Figure 4(b) shows the curvature and distortion, where the maximum distortion appears to be –0.904%; Fig. 4(c) shows the relative illumination being above 50%, the lowest 51.6%, within the maximum field of view.

Table 1. The specifications of CCD camera.

Sensor		
	Resolution	658 H × 492 V (VGA)
	Pixel size	9.90 µm × 9.90 µm
	Sensor area	6.52 mm × 4.89 mm
	Image height (H)	3.26 mm
	Image height (V)	2.45 mm
Lens		
	F number	2.8
	EFL	4.88 mm
	Horizontal half of FOV ($\theta_{\omega(H)}$)	24.8°
	Vertical half of FOV ($\theta_{\omega(V)}$)	17.6°

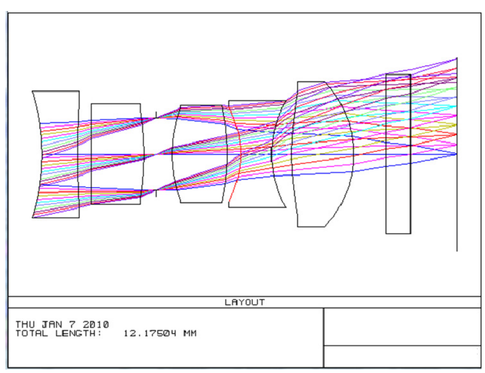

Fig. 3. Lens layout after optimization.

#185526 - $15.00 USD Received 19 Feb 2013; revised 21 Mar 2013; accepted 23 Mar 2013; published 29 Mar 2013

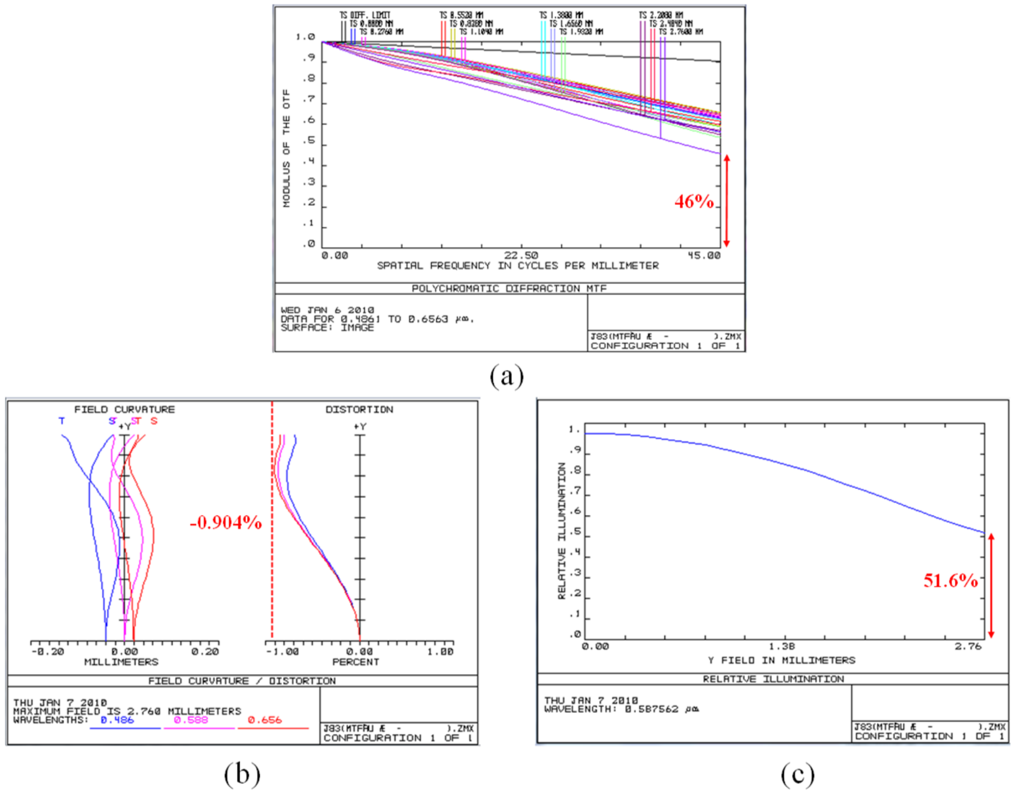

Fig. 4. Image quality of the lens: (a) MTF; (b) field curvature and distortion; and (c) relative illumination.

2.2 Double-symmetric prism design

In addition to the half-angle of view of the lens, the vertex angle of the prism is one of the factors in the collect cone angle of the system. With the proposed panorama stereo acquisition technique, cameras are placed every 20 degrees for panorama acquisition of the target, where each camera acquires images from four different angles of view, and the neighboring images are calculated as a panorama stereo image with IBR and binocular parallax. In this case, the less correlation that appears among the four images acquired by a camera, a clearer image layer of IBR is presented and the less crosstalk of binocular parallax is shown. From Eq. (1), the smaller the α, the smaller the δ_o, when the marginal ray is closer to the optic axis, so that the acquired images reveal less correlations. According to the present process, the horizontal vertex angle $\alpha_{(H)}$ of the prism is defined as 4.0°, and the vertical vertex angle $\alpha_{(V)}$ is 3.0°. The conditions of the horizontal angle of view $\alpha_{(H)}$ and $\theta_{\omega(H)}$ and the vertical angle of view $\alpha_{(V)}$ and $\theta_{\omega(V)}$ are substituted for Eqs. (1) and (2), respectively, for the four collection areas of the camera through the double-symmetric prism, as shown in Fig. 5. Figure 5(a) shows the collection areas acquired by the camera with the horizontal half-angle of view, in which the maximum width $\delta_{w(H)}$ appears to be 22.5° and the collect cone angle $\delta_{o(H)}$ of marginal ray 2.0°. Figure 5(b) shows the collection area of the camera with a vertical half-angle of view, in which the maximum width $\delta_{w(V)}$ is 16.0° and the collect cone angle $\delta_{o(V)}$ of the marginal ray is 1.5°.

Figure 6 shows the schematic diagram of the double-symmetric prism, where the pitch of the prisms with the horizontal angle of view is 21.45mm and the prisms with the vertical angle of viewprism is 28.62mm; the height of the prisms and the plate thickness are the same size as 1.5mm. With the optimization of lens, it is placed 30mm in front of the lens for

#185526 - $15.00 USD Received 19 Feb 2013; revised 21 Mar 2013; accepted 23 Mar 2013; published 29 Mar 2013

Soptimal image quality. Moreover, in consideration of the effects of prism dispersion on images, materials with larger Abbe numbers (V_d) are generally used for deleting color dispersion. Polymethylmethacrylate (PMMA, V_d = 57.4) therefore is selected as the material of the prism.

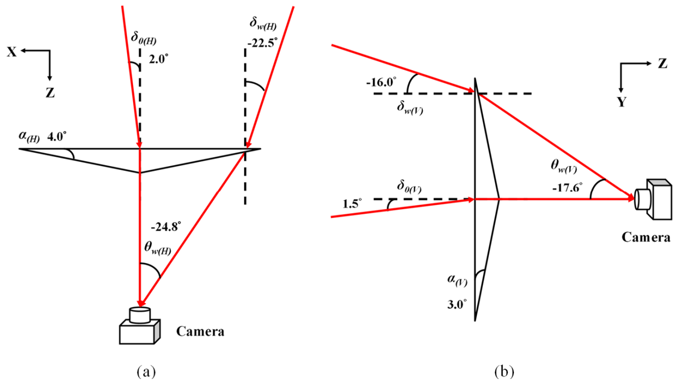

Fig. 5. The collection area of the half-angle of view of the symmetric prism camera: (a) Horizontal angle of view; (b) Vertical angle of view.

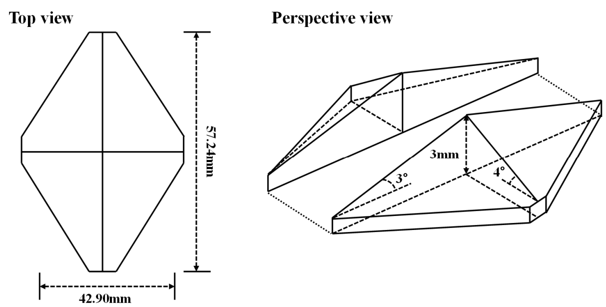

Fig. 6. Schematic diagram of the double-symmetric prism.

2.3 Panorama stereo image method

Figure 7 shows the panorama acquisition in the stereo acquisition system. Single-lens cameras are placed every 20 degrees to obtain the left and the right angles of view on the latitude axis and the upper and the lower angles of view on the longitude axis through the double-symmetric prism, presenting quadrants on the CCD. In other words, a camera could be regarded as four virtual cameras so that the image in the first quadrant presents the upper left angle of view, the upper right angle of view in the second quadrant, the lower right angle of view in the third quadrant, and the lower left angle of view in the fourth quadrant. According to the stereopsis of binocular parallax [1], the first quadrant acquired from odd cameras and the second quadrant acquired from even cameras could form stereo image pairs with the upper angle of view. Similarly, the fourth quadrant acquired from odd cameras and the third quadrant acquired from even cameras could form stereo image pairs with the lower angle of view. IBR is further utilized for calculating the quadrants acquired from the 18 cameras to 18 stereo image pairs [Fig. 8(a)]. Finally, the 18 stereo image pairs are linked as a panorama stereo image with the upper and the lower angles of view, as shown in Fig. 8(b).

#185526 - $15.00 USD   Received 19 Feb 2013; revised 21 Mar 2013; accepted 23 Mar 2013; published 29 Mar 2013

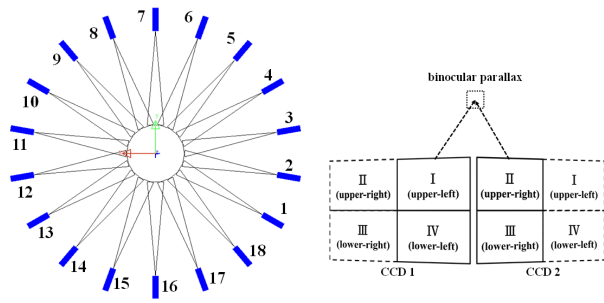

Fig. 7. Panorama acquisition of the 18 double-symmetric prism cameras.

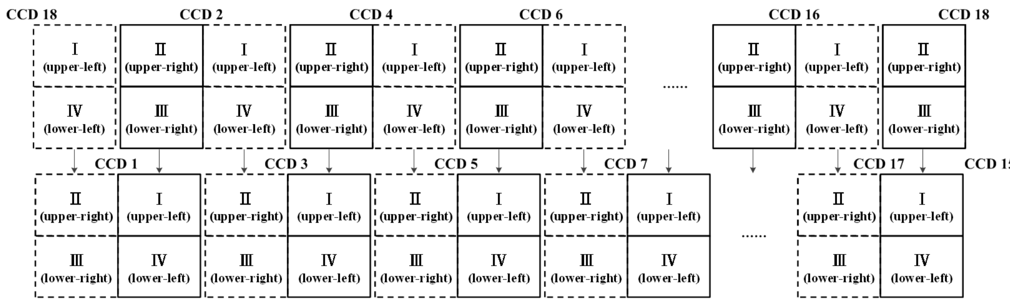

(a)

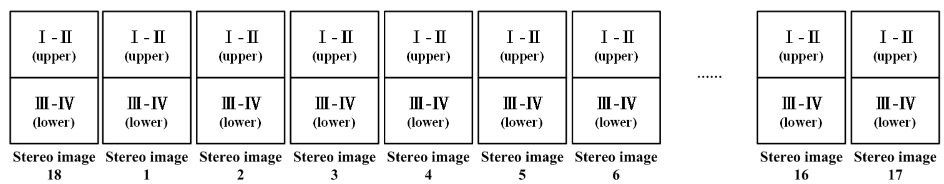

(b)

Fig. 8. (a)stereo image pairs processed by IBR; (b) panorama stereo image.

3. Experiments and analysis

After completing the double-symmetric prism (see Fig. 9), it is equipped in front of the designed lens for shooting. The results are shown in Fig. 10. Figure 10(a) shows the images without the double-symmetric prism; the image resolution appears 658 × 492 and the shooting distance 1000mm. Setting up a mark as the focus of the image, it would be the origin of the marginal ray. When the double-symmetric prism is placed in front of the lens, the original image is divided into a quadrant image with the mark in the original image being located in the four quadrants. The horizontal displacement distances 128dpi, while the vertical displacement distances 97dpi, as shown in Fig. 10(b). After the calculation of perspective projection theory [19], the horizontal displacement distances 34.98mm, and the vertical displacement 26.51mm. In other words, the angle between the horizontal marginal ray and the ray axis is 2.0°, and between the vertical marginal ray and the ray axis 1.5°. Such results correspond to the design.

#185526 - $15.00 USD Received 19 Feb 2013; revised 21 Mar 2013; accepted 23 Mar 2013; published 29 Mar 2013

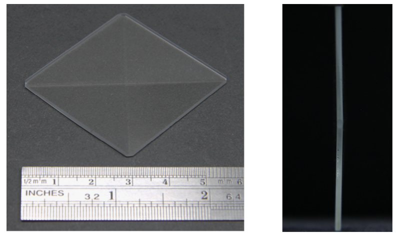

Fig. 9. The double-symmetric prism: (left) top of view, (right) right of view.

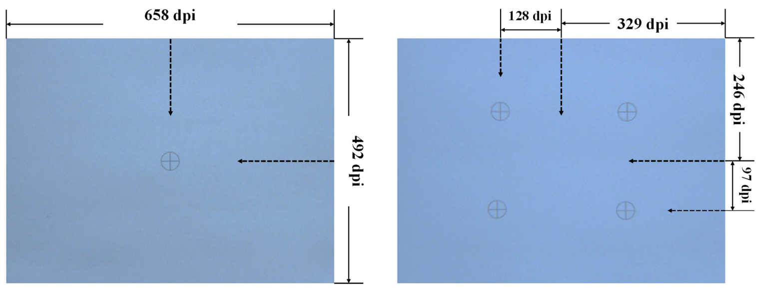

(a) (b)

Fig. 10. Test image with the double-symmetric prism camera (a) without the double-symmetric prism, (b) with the double-symmetric prism.

3.1 Analysis of stereogram

Figure 8(a) reveals the images acquired by two different cameras being combined into a stereo image pair with binocular parallax. The minimum disparity of the stereo image pair could be defined 1.99mm, according to the offset of the marginal ray passing the prism and the pixel size of CCDs. Such disparity could reflect the stereo depth of 57.70mm when an observer viewing the images with positive parallax (or negative parallax).

Figure 11 presents the images shot by the double-symmetric prism camera at 0° and 20°, with the distance 1000mm. In the figure, the first quadrant of camera 1 is combined with the second quadrant of camera 2 into a stereo image pair with binocular parallax by IBR. Similarly, the fourth quadrant of camera 1 and the third quadrant of camera 2 are combined, Fig. 12. With cyclopean vision [20], the stereo image in the figure would extrude the screen when the dot viewed by both eyes would be convergent to a point; besides, the positive parallax (or negative parallax) could be adjusted to determine the depth relationship of the object, with the depth about 38.63mm. Moreover, the distances of the upper and the lower objects would be different because of the distinct angles of view.

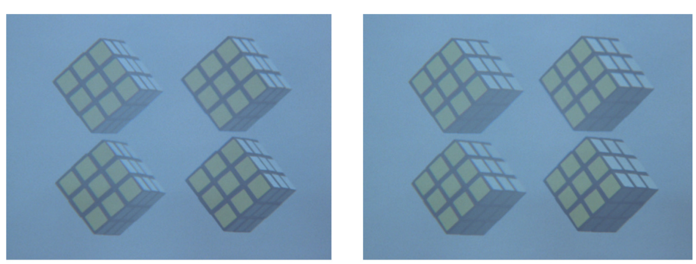

(a) (b)

Fig. 11. Quadrant images shot by the double-symmetric prism camera (a) camera 1 at 0°, (b) camera 2 at 20°.

#185526 - $15.00 USD Received 19 Feb 2013; revised 21 Mar 2013; accepted 23 Mar 2013; published 29 Mar 2013

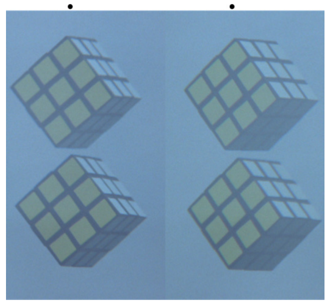

Fig. 12. Stereo image pair.

3.2 Panorama stereo image

After the above verification succeeded, the 18 double-symmetric prism cameras proceed with the panorama acquisition of the object, which is a 3D block. Having the cameras every 20 degrees take a quadrant image, the acquired quadrants are combined as a panorama stereo image with IBR, as shown in Fig. 13. From the figures, the panorama images acquired by the cameras could obtain the left and right image pairs from various angles of view of the object, and the upper and the lower angles of view can also be obtained for increasing the viewing area. Besides, there is no crosstalk between the left and the right images; nor is moiré effect in integral photography generated. Moreover, this study also precedes dynamic acquisition of the rotation of the object, and IBR is similarly utilized for combining a panorama stereo video (Media 1 and Media 2).

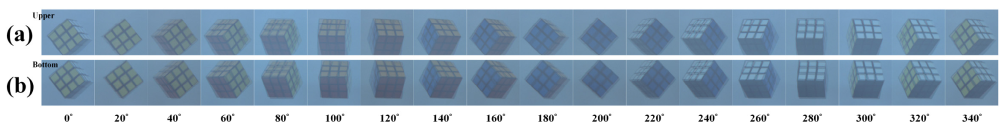

Fig. 13. The results of the panorama stereo image pair: (a) upper side of view; (b) lower side of view.

4. Conclusion

By combining single-lens cameras with the double-symmetric prism arranged by the prisms with the horizontal angle of view (the vertex angle 4°) and the vertical angle of view (the vertex angle 3°), four images from different angles of view can be received with one acquisition. Under the panorama acquisition from the cameras that are placed every 20 degrees, 18 quadrant images are acquired, in which two neighboring images with the left and the right angles of view correspond to the stereo image pair of binocular parallax. The panorama stereo image pair with the vertical angle of view ± 16 is then formed through image-based rendering. In comparison with traditional panorama acquisition technique, this study largely reduces the number of cameras and with merely 1/4 resolution, comparing it to integral photography, and the moiré effect does appear.

Acknowledgments

This work is supported by the National Science Council of Taiwan under contract no. NSC 100-2221-E-224-044-.